20XX-01-XXXX

Development of an autonomous battery electric vehicle

Author, co-author (Do NOT enter this information. It will be pulled from participant tab in MyTechZone)
Affiliation (Do NOT enter this information. It will be pulled from participant tab in MyTechZone)

Abstract

Autonomous vehicles have been shown to increase safety for drivers, passengers and pedestrians and can also be used to maximize traffic flow, thereby reducing emissions and congestion. At the same time, governments around the world are promoting the usage of Battery Electric Vehicles (BEVs) to reduce and control the emissions of CO2. This has made the development of autonomous vehicles and electric vehicles a very active research area and has prompted a significant amount of government funding.

This paper presents the detailed design of a low-cost platform for the development of an autonomous electric vehicle. In particular, it focuses on the design of the electrical architecture and the control strategy, tailored around the usage of affordable sensors and actuators. The specifications of the components are extensively discussed in relation to the performance target. The aim is to provide a comprehensive guide for the development of the remotely-controlled platform, in order to lower the entry barrier for the development of autonomous electric vehicles.

Introduction

Governments have been keen to promote the use of autonomous vehicles as they have the potential to reduce emission and congestion whilst improving safety. Drivers have been shown to have a significant effect on road accidents with accidents caused by lack of awareness (distracted etc., 41%), poor critical reasoning (too fast, misjudging other drivers' actions etc., 34%), poor driving (over and poor steering etc., 10%) and driver debilitation (falling asleep, heart attack etc., 7%) [1]. Autonomous vehicles therefore have a huge potential to reduce accidents but they may inadvertently introduce new types of risk due to their different perception and modelling of the world.

There are also issues in relation to technology, public acceptance and regulatory control. Governments are therefore looking to introduce pathways and legislation that will direct and control the implementation of autonomous vehicles [2]. Although autonomous vehicles have been shown to operate well with limited driver interaction the next stage will look to develop fully autonomous vehicles with technology road maps indicating implementation in 2025 and Google predicting 2017 [2]. Key areas of technology that need to be brought together and developed further are overall safe vehicle control (data and operation - braking, acceleration and steering), navigation, surroundings awareness and safe switching between direct and autonomous control.

A barrier to widespread implementation is developing autonomous vehicles at costs that are acceptable to the majority of consumers [3]. In addition, there is work on developing inter vehicle communication which has the potential to deliver better traffic management, improved safety through inter vehicle operability and improved information to drivers and passengers [4]. As well as technological issues there are also concerns about control security of autonomous vehicles (cyber-attack), public acceptance of autonomous vehicles and liability in cases of accidents [2].

To provide impetus for future technology, competitions such as the DARPA Grand Challenge [5] and Intelligent Future Vehicle Challenge in China have been set up. In preparation of the DARPA Urban Challenge 2007, as part of team Victor Tango, Patrick Currier converted a hybrid Ford Escape for autonomous control [6]. This project was the basis of his PhD in which he gives a detailed account of the vehicle design. More recently Zhao et al [7] presented work on adaptive PID control system for an autonomous vehicle called 'Intelligent Pioneer'. Some general information on the vehicle design is given. Although there are many news articles about autonomous vehicles being developed there is little information detailing their design and most designs seem to be based on modifying existing Internal Combustion Engines Vehicles (ICEVs) or hybrid vehicles.

BEVs have become more common [8] primarily driven by Government legislation [9] via awareness of the need to reduce pollution, and through manufacturers producing more viable BEVs with regard to price and mileage range. BEVs main advantages are their ability to reduce the amount of pollution that is generated within populated areas [10] and also to provide a quieter form of transport in comparison to ICEVs. It is also hoped that the introduction of BEVs will provide motivation to introduce more environmentally sustainable sources of electricity generation [11] reducing the overall CO2 and other harmful emissions produced.

BEVs also have the advantage over ICEVs in that the drive trains provide high torque, have a smaller amount of moving parts, are lighter and have simpler construction. For example, a YASA-400 electric motor can deliver 400Nm of torque and weighs 24kg [12] where as a General Motors ECOTEC 1.6L I-4 VVT (LDE) can deliver 155Nm of torque and weighs 116kg [13]. Vehicle manufactures have also claimed a 10% reduction in maintenance costs comparing BEVs to ICEVs [14]. A key area of reduction in the drive train is the removal of a clutch and gear box with electric motors being able to provide a constant torque over a range of speeds. Torque control of electric motors is also very quick, in the order of milliseconds, the torque can also be precisely measured and estimated and the low weight of electric motors enables the use of

multiple units giving the ability to independently control torque at each wheel [15, 16]. These three properties give control performance beyond what is achievable with ICEVs [17, 18] and allow technologies such as anti-lock braking, anti-slip regulation and electronic stability control to be integrated directly [19, 20].

The batteries are the key component that is limiting the use of BEV's [21, 22]. The batteries are costly, have low energy density (range), have long charging times [22, 23], have limited life and use materials that are not sustainable. In order to have a guaranteed range of 100km the cost of the battery is approximately $4000 per vehicle [24]. The energy density of batteries is approximately 16.6 times worse in terms of weight and 5 time worse in terms of volume [25, 26].

The good news is that battery technology has been rapidly evolving and concerns about safety and life time of lithium batteries have largely been solved. The estimated life of a battery in now estimated at 3000 charges or 10 years [14, 27]. Faster charging has also significantly reduced the time of charging [27, 28].

In this paper the design and development of an autonomous vehicle to be used as a test bed for inter vehicle communication, vehicle navigation, vehicle control and vehicle surrounding awareness is presented. In addition, an electric vehicle drive was chosen so that the control benefits of torque control at each wheel can be investigated.

Design Brief

The design requirements for the autonomous vehicle were set as

- Ability to manoeuvre across rough terrain
- Small enough to pass down narrow roads
- Be electrically driven
- Have the capacity to carry small loads and a driver
- Have at least two independently driven wheels
- Ability to stream video and commands wirelessly
- Ability to act autonomously

One of the ideas behind the brief was that the vehicle should be able to act as packhorse for someone. For instance, a gardener where the vehicle would follow the gardener around carrying his tools.

Design

Chassis

To meet the design brief of having a small but hardy vehicle for use on off road terrain it was decided to utilise an existing electric quad bike to provide the chassis for the new Autonomous Battery Electric Vehicle (ABEV). Therefore, a second hand Global Electric Motorcars Quadriga was purchased. The Quadriga Quad bike had 6 lead acid batteries powering a single motor that provided drive to the rear wheels through a gear box.

Batteries

Five of the six original lead acid batteries where used to provide power to the ABEV with four of them used in series to provide power for the drive motors and the steering motor and the fifth battery used for all the control circuitry. Each battery has a nominal voltage of 12V and a capacity of 75Ah.

Drivetrain

The single motor and the gearbox were replaced by two DC motors driving directly the two rear wheels, as shown in Figure 1. They were selected to provide 20Nm peak torque at the motor shaft for 110A of current. Each of them was connected directly to one of the two rear wheels through a 7.3 gear ratio, to allow for 146Nm of torque at each wheel. The two motors are controlled independently and this architecture could generate unintended yaw if one of the two wheels starts skidding. The design does not though incorporate traction control or torque vectoring, given that the vehicle doesn't have enough torque to reach high slip ratios in the expected conditions of usage, and therefore the yaw moment should be negligible and easily neutralized with small changes in the steering position.

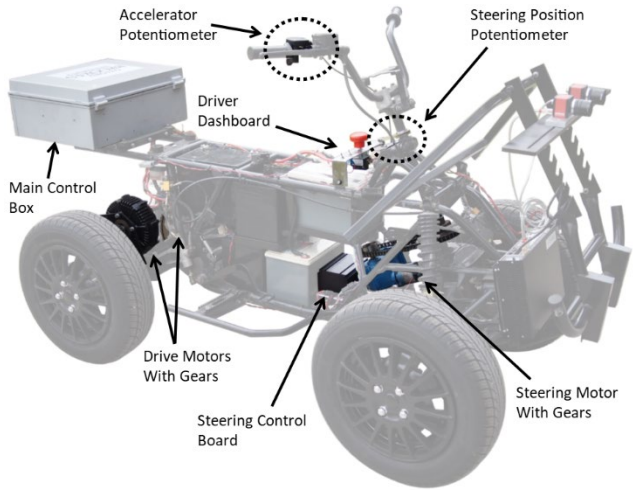

Figure 1: The quad bike at the end of the project.

Vehicle control

For the overall vehicle control a National Instruments CompactRIO was chosen, see Figure 2. This device can utilise a variety of add on modules that can read and send data, carry out high frequency computations and control actuators. The CompactRIO has a very rugged design which makes it suitable for vehicle application in which shocks and vibrations occur.

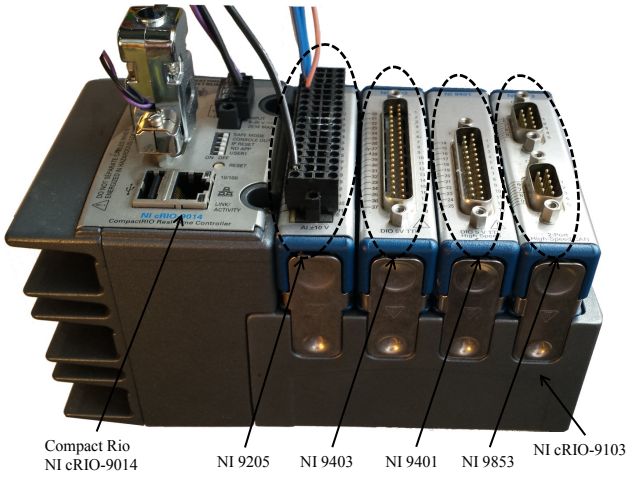

Figure 2: The CompactRIO and add-on-modules used on the ABEV.

The following CompactRIO and add-on-modules were used in the ABEV:

- NI cRIO-9014: 400 MHz Freescale MPC5200 processor, 2GB storage, 128 MB of DRAM, Ethernet port, USB port and one serial port [29, 30].
- NI cRIO-9103: 4-slot Field Programmable Gate Array (FPGA) [31].
- NI 9205: 32-channels, ±10V, 250 kS/s, 16-bit analog input module [32].
- NI 9403: 32-channels, 7 µs digital I/O module [33].
- NI 9401: 8-channels, 100 ns ultrahigh-speed digital I/O module [34].
- NI 9853: 2-port high-speed CAN module [35].

The NI cRIO-9014 is used as the main controller and data gateway. In autonomous mode, it reads the torque commands and the steering commands from the Ethernet port and converts them into targets for the current controller, implemented in the NI 9103 (see section on drive motor control hardware), and the steering control board (see section on steering control hardware). In manual mode, it is used to generate the target for the current controller from the position of the potentiometer. It is also used to communicate with the IMU and to compute the mechanical dynamics of the ABEV, as well as to store all data into non-volatile memory, for logging purposes. The NI 9205 is used to sample the battery voltage, the potentiometer voltages (see section on steering control hardware) and the current from the two drive motors (see section on drive motor control hardware). The NI 9403 is used to read inputs from the driver dashboard, such as the desired direction of motion (forward or backward), and to control the relays of the vehicle. The NI 9401 is used to send the pulse width modulation (PWM) signals to the drive motor controller (see section on drive motor control hardware). The NI 9853 is used to communicate with the steering control board (see section on steering control hardware). Figure 3 shows all the electrical connection of the CompactRIO, apart from the wireless router (connected via Ethernet), and the IMU (connected via serial port).

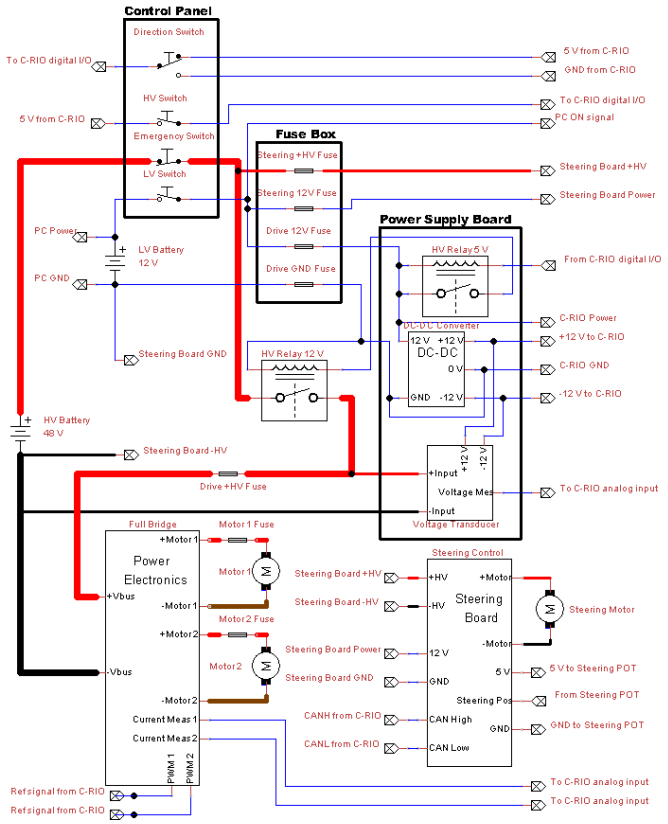

Figure 3: Electrical schematics of the vehicle, excluding the CompactRIO, the wireless router and the IMU.

Steering Motor

In order to determine the torque required for the steering several tests were carried out measuring the input torque from drivers with the quad bike moving and whilst stationary. From this a torque of approximately 200Nm with a speed of approximately 2rpm was decided upon as realistic values to aim at. A person could turn the steering quicker than this but having a very fast steering was not deemed necessary for the applications that the ABEV was intended for. The motor selected for the steering was a Parvalux PM10 with LWS gearbox providing 0.2Nm of continuous torque for a current of 2A, and 0.3Nm of peak torque for a current of 3A. The motor shaft was directly connected to a worm gear providing a gear ratio of 1:833. This does cause a high loss with 100W of electrical power giving only 50W of mechanical power but does increase the peak torque to 125Nm. The worm gear offers the advantage of only allowing drive to go from the input shaft to the output shaft [36] as well as a small form factor. The output shaft of the worm gear has a gear sprocket which is connected to a gear sprocket on the steering by a drive chain, giving a further gear ratio of 1:2.2. This gives a final torque at the steering column of 275Nm for a rotational speed of 1.7rpm (50W/275Nm*30/π).

Steering Motor Control

Steering Control Hardware

In order to measure the steering direction a Vishay Spectrol 357-4506-502 rotary potentiometer with a gear attached was connected to a gear on the steering column via a toothed belt, providing a gear ratio of 1:2.5. This meant that turning the steering column 136º caused one full rotation of the potentiometer.

Metal-oxide-semiconductor field-effect transistors (MOSFETs) were chosen to handle the higher power switching to drive the motor. As the motor needs to operate in both directions, four MOSFETs were used in an H bridge configuration to control the voltage to the motors. This method applies different width voltage pulses to modulate (PWM) the average voltage between 0 V and the battery voltage.

To control the steering motor, a PCB has been designed as shown in Figure 4. The board has a Microchip PIC18F4580 microcontroller which controls the position, the Controller Area Network (CAN) communication and the PWM. The four big pads visible on the Printed Circuit Board (PCB) are the connections for the 48V supply and the motor terminals. Their size is large as the PCB was designed to control currents up to 50 A. This was to future proof the design to enable it to be used with a variety of motors. The steering motor on the ABEV would only need to draw a maximum current of 3A. Other inputs to the PCB are the CAN bus, four analogue inputs and the power for the control electronics. The power to the board is taken from the 12V single battery and converted on the board to 5V to power the microcontroller.

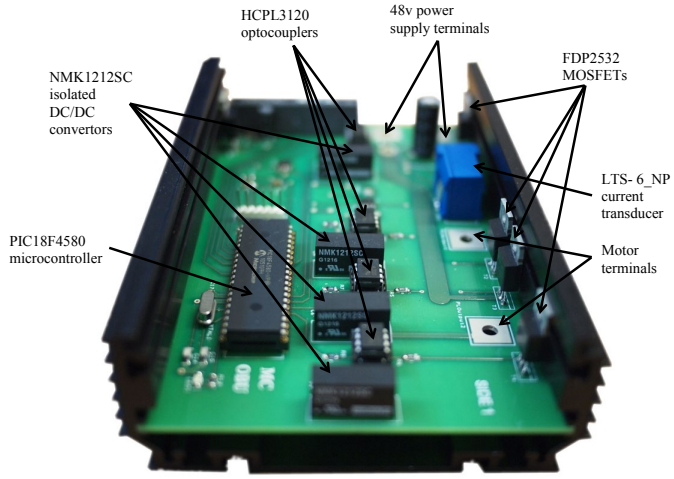

Figure 4: Steering control PCB and components mounted in protective case.

Steering Control Code

The control code was written in C language and compiled using MikroC compiler for Microchip peripheral interface controller (PIC). The conventional approach uses three control loops to control steering position, steering speed and motor current (torque) [37, 38]. Unfortunately, the steering speed cannot be measured with enough accuracy due to hardware limitations, and so the conventional method cannot be used. The steering position is measured using a potentiometer, which gives 5 volts output for a full turn of the potentiometer (136º rotation of the steering column), which means the output voltage of the potentiometer is 37mV/º. The analogue to digital convertors have a resolution of about 5mV which represents about 1/8º. The speed of the motor is slow, around 10º/s (1.7rpm), which means that it would take over 10ms before this movement is detected and as this movement is small the output voltage generated will be masked by background electromagnetic noise and vehicle vibrations. To accurately predict the steering speed, measurements would need to be taken over hundreds of milliseconds, which would introduce an unacceptable response delay in the control system.

The steering control was therefore designed to just use the position and motor current as inputs, see Figure 5. The rate of voltage increase/decrease to the motor is set with a control parameter. If the current limit is exceeded, the voltage is reduced by the set value. When the current is within normal values and there is a positive error in steering position the voltage is increased by the set value, making the motor turn forward which reduces the error, and when there is a negative error in steering position the voltage is decreased by the set value, making the motor turn backwards which reduces the error. The code checks the inputs every millisecond, which is fast enough to suppress any critical overcurrent. The disadvantages of the control system implemented are that it has a slow response time and a non-zero steady state error but given the slow speed of the motor such loss in performance is not appreciable and the steady state error is within a couple of degrees. The steering control system on reading the set position sends back to the overall vehicle controller, through the CAN bus, the actual position. This is to provide feedback to help control the path of the vehicle and also to make sure that if the steering is stuck, e.g. because the wheel is in a rut, that the steering control is not trying to run at full torque which could cause overloading of the motor.

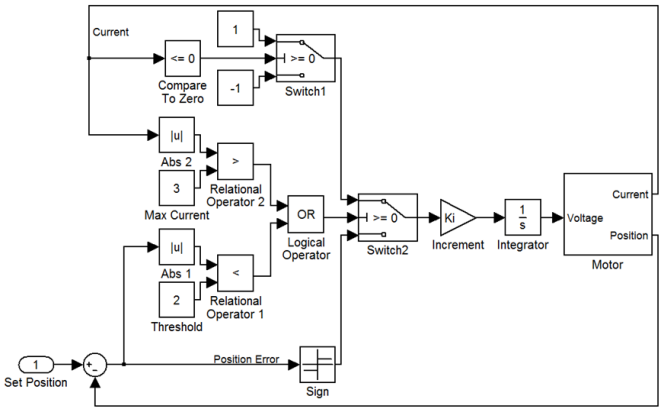

Figure 5: Steering position control system.

Drive Motor Control

Drive Motor Control Hardware

For a permanent magnet Direct Current (DC) motor the torque can be considered with reasonable accuracy to be proportional to the DC current. As the current can be more easily measured than the torque, it was decided to control the torque by controlling the current. The torque generated by the motors in relation to current is 0.18Nm/A giving a torque of 1.32Nm/A at the wheel. While commercial motor controllers were available, none of them offered a user programmable fast and responsive torque control, in the order of a few milliseconds, which was required to enable development of advanced features like slip estimation. For this reason, a bespoke controller was developed.

A similar H bridge MOSFET configuration was utilised as for the steering control but in this case higher power MOSFETs IXFN 150N15 were used which can handle a current of 100A. In this case, as there are two drive motors, eight MOSFETs in total were used. These were paired and mounted below the developed PCBs. Each PCB has a current sensor and protection from overcurrent.

Optocouplers, powered by a separate DC to DC convertor, are used to drive the MOSFETs. This ensures that the voltage sources used by the control electronics and used by the drive motors are isolated from each other. The optocouplers drive the gate between +12V and -12V. The negative voltage is used to prevent the MOSFET turning on suddenly due to voltage oscillations at the gate [39]. Overcurrent protection is achieved by short circuiting the optocoupler whenever an overcurrent is detected. The maximum positive and minimum negative currents can be adjusted using potentiometers on the board. The batteries (48V) are connected to the PCBs using thick copper plate, designed to handle the high currents the motors require. A capacitor is connected in parallel with the 48V bus to filter the oscillations caused by the PWM and a fuse is in place to protect the battery from short circuit. The motors are also protected with fuses. Figure 6 shows the main control circuitry for the ABEV.

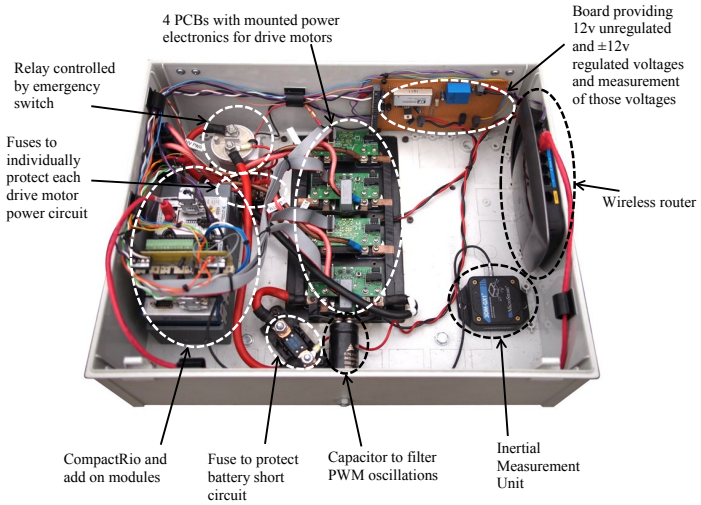

Figure 6: Main control box for the ABEV showing CompactRIO (plus modules), DC to DC convertor, drive motor PCBs, Wi-Fi router and Inertial Measurement Unit (IMU).

As the current is being used to control the torque, any oscillations in the current generate oscillations in the torque. It is therefore important to reduce the current ripple amplitudes, which can be achieved by increasing the PWM frequency. A 20kHz PWM frequency was used on the ABEV (50µs pulse period). The PWM signal for setting the voltage is controlled by the FPGA clock in the NI cRIO-9103 (40MHz), which means the PWM signal could be set with an accuracy of 25ns. However, the update rate of the NI 9401 is only 100ns [34], which limits the resolution of the duty cycle that can be applied. This translates into a resolution of the average voltage applied across a PWM cycle, which is the control variable, of 0.096V (100ns/50µs×48V). This resolution is relatively high and allows for a stable current control.

The need for analog overcurrent protection was driven by the low values of the armature inductance (20µH) and resistance (45mΩ), which means that the current could rise to damaging values more quickly than the controller can respond (50µs).

Drive Motor Control Tuning

The control consists of a discrete implementation of a proportional integral (PI) controller with the output limited to the battery voltage. The discrete transfer function between the motor voltage and current is given by Equation (1).

$$G_p(s) = \frac{\frac{1}{L_a}}{s + \frac{R_a}{L_a}} \qquad (1)$$

where s is the Laplace operator, La is the armature inductance and Ra is the armature resistance.

The discrete model of the motor can be obtained by the z-transform of the product of Gp(s) and the Laplace function of a zero-order hold [40] as expressed by Equation (2).

$$G_p(z) = \text{z-transform of } \mathcal{L}^{-1}\left(\frac{1 - e^{-2sT_{PWM}}}{s} \cdot \frac{\frac{1}{L_a}}{s + \frac{R_a}{L_a}}\right) = \frac{1 - e^{-2\frac{R_a}{L_a}T_{PWM}}}{R_a\left(z - e^{-2\frac{R_a}{L_a}T_{PWM}}\right)} \qquad (2)$$

where T_{PWM} is the PWM time period.

Substituting the motor inductance, motor resistance and PWM time period into Equation (2) gives Equation (3).

$$G_p(z) \approx \frac{4.47}{z - 0.79} \qquad (3)$$

Using Matlab and the function *pidtune* the gains for the PI controller were calculated by selecting a desirable response time which did not compromise the stability of the system. The gains obtained were 0.002 for the proportional gain and 40 for the integral gain. The theoretical time to settle was in the order 5ms with an overshoot of 5%. This speed of response enables control of the current up to frequencies of 50Hz.

Drive Motor Control Code

The Compact Rio FPGA enables fast simultaneous processing of multiple tasks. It has limitations though in terms of control code size that can be embedded, libraries and operations available, the need to compute within one clock cycle etc. Its speed of operation does though make it very suitable for motor drive control. LabVIEW, a visual programming language developed by National Instruments, was used to create the control code. The code developed is split into three main blocks dealing with the CAN communication, the drive motor current control and the generation of the PWM signal. Figure 7 shows the top-level structure of the FPGA code.

The block for the CAN communication is split into two sections. In the first section, the CAN communication code waits for read and write triggers from the CompactRIO microprocessor. In the second section, the code writes or reads data according to the trigger. A check is made on whether the communication has been successful and this will loop until the communication is successful. Error messages are written so that the microprocessor is aware of the communication status.

The block for the motor current control is also split into two sections. In the first section, the program simply waits for the beginning or the midpoint of the PWM cycle before going to the second section of

code (reason discussed later). In the second section the currents are sampled, the overcurrent is checked, the voltages for the motors are determined (PI control), the set voltages are converted to PWM data and the data is written into the First In First Out (FIFO) data storage.

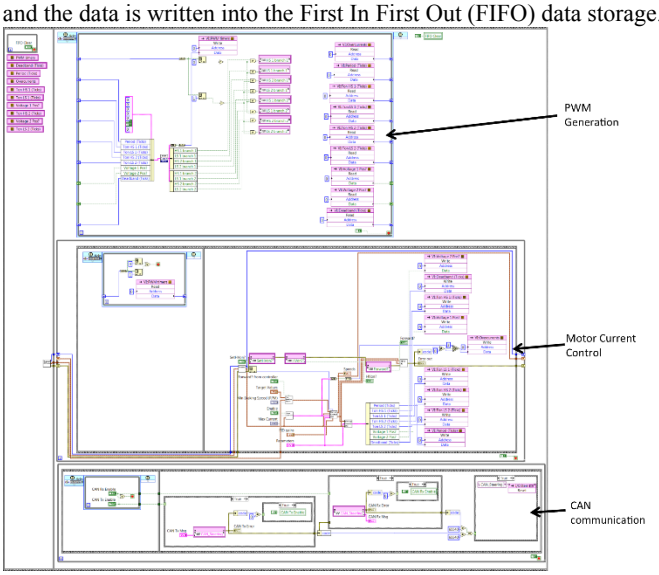

Figure 7: The top-level structure of the code in the FPGA.

In each leg of the H bridge the two MOSFETs switch in opposition to pull the voltage at the motor drive terminal from positive voltage (+48V) to zero (or vice versa). Due to the time required to switch the transistor from on to off a short circuit can be temporarily created across the bridge. To avoid this, deadband periods are introduced, during which time both transistors are controlled to be off.

The motor current is roughly proportional to the voltage difference between the applied motor terminal voltage and the back electromotive force voltage. During the deadband periods the motor current is sustained by freewheeling diodes contained within the MOSFETs. During each PWM period the transistors are switched twice (on/off or vice versa) so there are two deadband periods per PWM period. During the deadband period the voltage seen at the motor terminals will be zero if the electromotive motor current generated is positive (accelerating) and will be the battery voltage if the electromotive motor current is negative (braking). The deadband period chosen was 1µs and with a PWM period of 50µs this gives a total deadband period per PWM cycle of 1/25th. This translates into a minimum voltage of 1.92V over the PWM cycle when the vehicle is slowing (braking).

To slow the motors down the drive motor controller will reduce the applied motor terminal voltage until it goes below 1.92V at which point due to the deadbands the controller will not be able to apply the appropriate voltage. To overcome this, the controller is cycled from 0 to 2V over several PWM cycles to try to give an average voltage close to the set value from the controller. This though can cause 30A oscillations in the current so instead it was decided not to use power braking when the speeds are low (controller set voltage not applied). In order to provide a more consistent driving experience rather than using voltage as a limit it was decided to use speed so that power braking ceases at the same speed each time.

In the block for the PWM generation the target PWM period, duty cycle (fraction of PWM period that battery voltage is applied to the motor terminals) and deadband data are read from the drive motor control block and converted into logic states for digital output. The current overload trip data is also received and the PWM signal is not sent if an overload has occurred. Finally, it sends triggers back to the drive control block in order to alternately sample the current at the beginning and middle of each cycle. The reason for doing this is that the switching of the MOSFETs during each PWM period causes the current to rise and fall, producing a drive motor triangular pulse shape. In order to calculate the average current a reading therefore needs to be taken at the beginning or towards the middle of each PWM cycle [41]. The NI 9205 analog input module can handle 16 differential inputs. Due to multiplexing the 250kS/s total sampling speed only gives a maximum of 15.625kS/s per differential input. As the PWM period is 50µs, a sampling speed of 20kS/s would be required to sample the currents twice within each PWM. This is not possible and so the currents are sampled over two cycles with the sampling speed of each input channel set to 10kS/s. The two motor currents, the battery voltage and the position of the potentiometer on the steering control are therefore all measured at a frequency of 10kHz.

Figure 8 shows the performance of the implemented current control. The plot starts with the vehicle accelerating from rest, then braking with maximum regenerative torque, then re-accelerating as soon as the braking torque drops due to the low speed threshold (as described above), and finally decelerating to rest. The current control is consistently robust, despite noticeable oscillations in the current due to the low inductance of the DC motor.

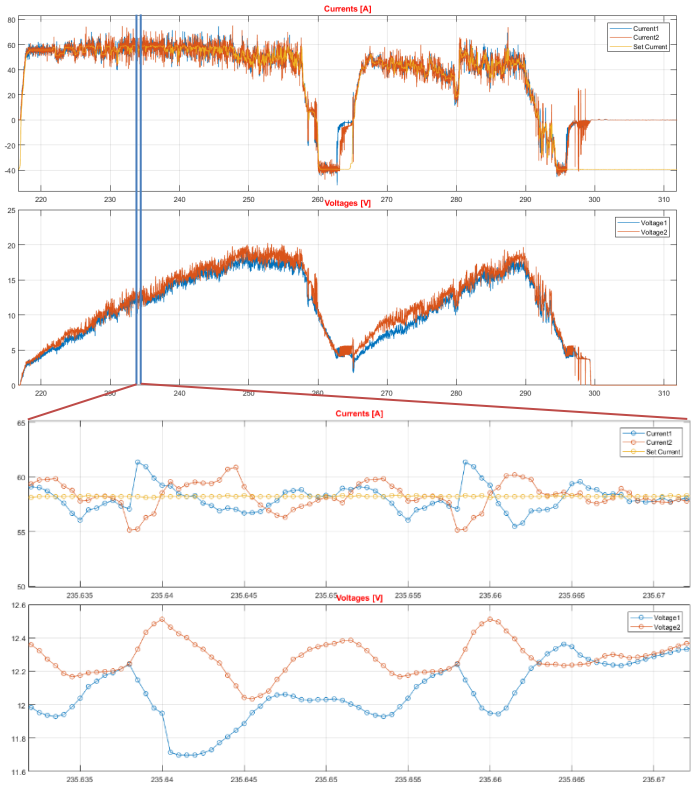

Figure 8: Recorded data showing the performance of the current control and the corresponding voltage (control variable) applied to the two drive motors. The second frame shows a magnification of the same data. The measurements have been downsampled to 2kHz.

Testing

The ABEV was developed to provide a test bed for inter vehicle communication, vehicle navigation, vehicle control, vehicle surrounding awareness and for developing torque control applications

such as slip control. To test some of the functions, such as drive control and wireless communication, the ABEV has been remotely controlled, see Figure 9. Tests have also been performed on remote steering using streamed stereo video sent back from the ABEV to the control centre. On board steering based on stereo video has also been tested. A technique has also been developed to determine the slip ratio by using low amplitude high frequency torque oscillations on top of the normal driving torque. The initial results of the work have been presented by Cecotti et al [42].

Figure 9: ABEV being remotely controlled.

Conclusions

An ABEV has been developed to provide a platform for testing autonomous technology. The chassis for the ABEV utilised a Global Electric Motorcars Quadriga quad bike which was modified to have two independent motors driving the rear wheels. Four lead acid batteries were used to provide power to the drive and steering motors, with a fifth battery used for the control circuitry. The vehicle was controlled using a CompactRio, NI cRIO-9014, with the following additional modules: NI cRIO-9103, NI 9205, NI 9403, NI 9401 and NI 9853.

The steering torque achieved was 220Nm for a rotational speed of 2.2rpm using a Parvalux PM10 motor with a LWS gearbox connected to a worm gear. Due to limitations with the hardware chosen, the steering control was written to only utilise the steering position, which was determined using a Vishay spectral rotary potentiometer rather than the more conventional method of using the steering speed with motor current control. Four MOSFETS in an H bridge configuration were used to control the voltage to the motors using PWM. A PCB incorporating a PIC18F4580 microcontroller was designed to control the steering position, CAN communications and the PWM. The disadvantage of the control system is that it has a slow response time, and a non-zero steady state error. The loss of performance is negligible though, given the slow motor speed, and the steady state error is within a few degrees of the correct answer.

The rear drive motors selected were Perm Motor PMG 132s. Utilising gear chains the maximum torque achieved at each wheel was 146Nm. This gives a driving force of 1081N for the 270mm wheels at a current of 110A per motor. The torque control was implemented by controlling the motor current. To enable slip estimation a fast responsive torque control in the order of a few milliseconds was necessary, which required the development of a bespoke controller. Similar H bridge MOSFET configurations were employed as used for the steering control, but this time utilising high power IXFN 150N15 MOSFETS. Due to the time required to switch the transistor from on to off a short circuit can be temporarily created across the bridge. To avoid this, deadband periods were introduced, during which time the controller set voltage is not applied to the motor. This though can cause 30A oscillations in the current when using power braking at low speeds. To prevent this and to provide a consistent feel to the driver, power braking was stopped when the speed dropped below a set value. Optocouplers were used to isolate the voltage used for the control circuits from the drive motors. A capacitor was used to filter the oscillations generated by the PWM, and fuses were put in to protect the battery and the motors. The minimum voltage that could be applied by the controller is 0.096V, set by the PWM frequency (20kHz), the battery voltage (48V) and limitations within the I/O module (PMW could only be set every 100ns). Due to the low armature inductance (20μH) and resistance (45mΩ) damaging levels of current could be generated more quickly than the controller could respond (50μS). Overcurrent protection was therefore incorporated through short circuiting the optocouplers whenever an overcurrent is detected. The proportional and integral gain of the motor controller was set to be 0.002 and 40 respectively, found using MATLAB and the function pidtune.

Initial work has demonstrated the usefulness of the ABEV with studies underway investigating autonomous vision, inter-vehicle communication and torque slip control.

References

1. NHTSA, “National Motor Vehicle Crash Causation Survey”, DOT HS 811 059, (DOT, 2008)
2. Pawsey, A., and Nath, C., “POSTnote 443 - Autonomous Road Vehicles”, (Parliamentary Office of Science & Technology, UK, 2013)
3. Lari, A., Douma, F., and Onyiah, I., “Self-Driving Vehicles and Policy Implications: Current Status of Autonomous Vehicle Development and Minnesota Policy Implications”, *Minnesota Journal of Law*, *Science & Technology*, 2015, **16**, (2), pp 735-769
4. Javadi, M. S., Habib, S. and Hannan, M. A., “Survey on Inter-Vehicle Communication Applications: Current Trends and Challenges”, *Information Technology Journal*, 2013, **12**, pp 243-250
5. “DARPA Grand Challenge”, http://www.darpa.mil/grandchallenge/index.asp, accessed on 2 October 2010
6. Currier, P. N., “VictorTango Architecture for Autonomous Navigation in the DARPA Urban Challenge”, *Journal of Aerospace Computing, Information and Communication*, 2008, **5**, (12), pp 506-529
7. Zhao, P., Chen, J., Song, Y. et al., “Design of a Control System for an Autonomous Vehicle Based on Adaptive-PID”. *Int. J Adv Robotic Systems*, 2012, **9,** (44)
8. Chan, C. C., and Wong, Y. S., “The State of the Art of Electric Vehicles Technology”, presented at International Power Electronics and Motion Control Conference (IPEMC), Xi’an, China, August 2004, pp. 46–57
9. Wansart, J., and Schnieder, E., “Modelling market development of electric vehicles”, presented at IEEE International Systems Conference, San Diego, USA, April 2010, pp. 371–376
10. Hodkinson, R., and Fenton, J., “Lightweight Electric/Hybrid Vehicle Design”, (Butterworth-Heinemann Ltd, 2001)
11. Husain, I., “Electric and Hybrid Vehicles: Design Fundamentals”, (CRC Press, 2010)

12. "YASA Motors Website", http://www.yasamotors.com, accessed on 3 September 2015
13. "GM Powertrain Website", http://gmpowertrain.com, accessed on 2 January 2013
14. Duleep, G., van Essen, H., Kampman, B., and Grünig, M., "Impacts of Electric Vehicles - Assessment of electric vehicle and battery technology", (CE Delft, 2011)
15. Sakai, S., Sado, H., and Hori, Y., "Motion Control in an Electric Vehicle with Four Independently Driven In-Wheel Motors", 1999, *IEEE Transactions on Mechatronics*, **4**, (1), pp. 9–16
16. Shino, M., Miyamoto, N., Wang, Y.-Q., and Nagai M., "Traction Control of Electric Vehicles Considering Vehicle Stability", presented at 6th International Workshop on Advanced Motion Control, Nagoya, Japan, April 2000, pp. 311–316
17. Fujimoto, H., Fujii, k., and Takahashi, N., "Vehicle Stability Control of Electric Vehicle with Slip-ratio and Cornering Stiffness Estimation", presented at IEEE International Conference on Advanced Intelligent Mechatronics, Zurich, Switzerland, September 2007, pp. 1 –6
18. Hori, Y., "Future Vehicle Driven by Electricity and Control - Research on Four-Wheel-Motored", *IEEE Transactions on Industrial Electronics*, 2004, **51**, (5), pp. 954–962
19. Hori, Y., Toyoda, Y., and Tsuruoka, Y., "Traction Control of Electric Vehicle: Basic Experimental Results Using the Test - EV UOT Electric March", *IEEE Transactions on Industry Applications*, 1998, **34**, (5), pp. 1131–1138
20. Sado, H., Sakai, S., and Hori, Y., "Road Condition Estimation for Traction Control in Electric Vehicle", presented at IEEE International Symposium on Industrial Electronics (ISIE), Bled, Slovenia, July 1999, **2**, pp. 973–978
21. Ehsani, M., Gao, Y., and Emadi, A., "Modern Electric, Hybrid Electric, and Fuel Cell Vehicles: Fundamentals, Theory, and Design", (CRC Press, 2nd edn., 2009)
22. Khan, I., "Emerging Technologies in Automobiles", presented at International Conference on Emerging Technologies, Peshawar, Pakistan, November 2006, pp. 368–377
23. Larminie, J., Lowry, J., "Electric Vehicle Technology Explained", (Wiley, 2003)
24. "Autoblog", http://www.autoblog.com/2015/10/08/gm-li-ion-battery-cost-per-kwh-already-down-to-145, accessed 8 June 2016
25. "XALT Energy", http://www.xaltenergy.com/index.php/solutions/technology/cells, accessed 8 June 2016
26. Thomas, G., "Overview of Storage Development DOE Hydrogen Program". presented at US DOE Hydrogen Program 2000 Annual Review, San Ramon, USA, May 2000
27. Grahn, P., and Söder, L., "The Customer Perspective of the Electric Vehicles Role on the Electricity Market", 8th presented at International Conference on the European Energy Market (EEM), Zagreb, Croatia, May 2011, pp. 141–148.
28. Grünig, M., Witte, M., Boteler, B., et al., "Impacts of Electric Vehicles - Assessment of the future electricity sector", (CE Delft, 2011)
29. "NI CompactRIO High-Performance Real-Time Controllers", http://www.ni.com/datasheet/pdf/en/ds-201, accessed on 7 September 2017
30. "NI cRIO-9012/9014", http://www.ni.com/pdf/manuals/374126g.pdf, accessed on 7 September 2017
31. "NI cRIO-9101/9102/9103/9104", http://www.ni.com/pdf/manuals/371559c.pdf, accessed on 7 September 2017
32. "NI 9205", http://www.ni.com/pdf/manuals/378020a_02.pdf, accessed on 7 September 2017
33. "NI 9403", http://www.ni.com/pdf/manuals/374069a_02.pdf, accessed on 7 September 2017
34. "NI 9401", http://www.ni.com/pdf/manuals/374068a_02.pdf, accessed on 7 September 2017
35. "NI 9853", http://www.ni.com/pdf/manuals/371453e.pdf, accessed on 7 September 2017
36. Norton, R., "Design of Machinery: And Introduction to the Synthesis and Analysis of Mechanisms and Machines", (McGraw-Hill Higher Education, 2008)
37. Craig, J. J., "Introduction to Robotics: Mechanics and Control", (Prentice Hall, 3rd edn. 2008)
38. Spong, M. W., Hutchinson, S., and Vidyasagar, M., "Robot Modelling and Control", (Wiley, 2005)
39. Wu, F., Gao, H., Sun, L., et al., "Suppression of Gate Oscillation of Power MOSFET with Bridge Topology", presented at 6th World Congress on Intelligent Control and Automation, Dalian, China, 2006, pp. 8196–82
40. Bolton, W., Control engineering, (Longman, 1998)
41. Bose, B.K., "Power electronics and variable frequency drives: technology and applications", (Wiley-IEEE Press, 1997)
42. Cecotti, M., Larminie, J., and Azzopardi, B., "Estimation of Slip Ratio and Road Characteristics by Adding Perturbation to the Input Torque", presented at ICVES, Istanbul, Turkey, July, 2013

Contact Information

neil.fellows@brookes.ac.uk
DR N Fellows, Department of Mechanical Engineering and Mathematical Sciences, Oxford Brookes University, Wheatley Campus, Wheatley, Oxford, OX33 1HX, UK

Acknowledgments

The authors would like to thank Walter Sweeting and the Departmental Workshop for the initial work on converting the Quad bike to utilize two electric motors, Sunando Sengupta and Michael Sapienza for the vision control development, Cristian Roman for work on wireless communication, Steve Barker for robotics input and to all their associated supervisors. The authors would also like to thank Professor William Clocksin for the original vision for the project and Professor Phillip Torr for carrying that vision forward.

Definitions/Abbreviations

ABEV	Autonomous Battery Electric Vehicle
BEV	Battery Electric Vehicle
CAN	Controller Area Network
CO2	Carbon dioxide
DARPA	Defense Advanced Research Projects Agency
DC	Direct current
FPGA	Field Programmable Gate Array
Gp(s)	Discrete transfer function
ICEV	Internal combustion engine vehicle
La	Armature inductance
NI	National Instruments
PIC	Peripheral interface controller
PCB	Printed circuit board
PhD	Doctorate in philosophy
PI	Proportional integral
PWM	Pulse width modulation
Ra	Armature resistance
s	Laplace operator
T_{PWM}	Pulse width modulation time period
MOSFET	Metal-oxide-semiconductor-field-effect-transistor